JACS
JOURNAL OF THE AMERICAN CHEMICAL SOCIETY

COMMUNICATION

pubs.acs.org/JACS

# Catalytic Activity Trends of Oxygen Reduction Reaction for Nonaqueous Li-Air Batteries

Yi-Chun Lu,[†,⊥] Hubert A. Gasteiger,[*,‡,⊥,§] and Yang Shao-Horn[*,†,‡,⊥]

[†]Department of Materials Science and Engineering, [‡]Department of Mechanical Engineering, and [⊥]Electrochemical Energy Laboratory, Massachusetts Institute of Technology, 77 Massachusetts Avenue, Cambridge, Massachusetts 02139, United States

Supporting Information

**ABSTRACT:** We report the intrinsic oxygen reduction reaction (ORR) activity of polycrystalline palladium, platinum, ruthenium, gold, and glassy carbon surfaces in 0.1 M $LiClO_4$ 1,2-dimethoxyethane via rotating disk electrode measurements. The nonaqueous $Li^+$-ORR activity of these surfaces primarily correlates to oxygen adsorption energy, forming a "volcano-type" trend. The activity trend found on the polycrystalline surfaces was in good agreement with the trend in the discharge voltage of Li-$O_2$ cells catalyzed by nanoparticle catalysts. Our findings provide insights into $Li^+$-ORR mechanisms in nonaqueous media and design of efficient air electrodes for Li-air battery applications.

Rechargeable Li-air batteries have the potential to provide 3−5 times the gravimetric energy density of conventional Li-ion batteries.[1−3] To make Li-air batteries practical for commercial applications, many issues[4,5] still need to be addressed, including low electrolyte stability, poor round-trip efficiency, rate capability, and cycle life.

Research efforts toward better understanding of the oxygen reduction reaction (ORR) mechanism and the design principles of highly active ORR catalysts are critical to improve the discharge performance, which directly affects the deliverable gravimetric energy and power of Li-air batteries.[4,6] Nanometer-scale catalysts based on precious metals (Au, 2.8 $V_{Li}$ at 100 mA $g^{-1}_{carbon}$ or 0.04 mA $cm^{-2}_{geo}$;[7] Pd, 2.87 $V_{Li}$ at 0.12 mA $cm^{-2}_{geo}$[8]) are reported to have higher discharge voltages than metal oxides (e.g., $\alpha$-$MnO_2$, 2.75 $V_{Li}$ at 70 mA $g^{-1}_{carbon}$;[2] $Fe_2O_3$, 2.6 $V_{Li}$ at 70 mA $g^{-1}_{carbon}$[9]). However, it is difficult to correlate reported geometric and carbon-mass-normalized currents of these catalysts to the intrinsic ORR activity such as true-surface-area-normalized ORR currents and ORR catalyst-mass-normalized currents of these catalysts. This is because the catalyst particle sizes and catalyst loadings can be significantly different among these studies. Further complication arises from the fact that carbonate-based electrolytes used in these studies[2,7−9] are unstable against ORR reaction intermediates such as superoxide ($O_2^-$) and form species such as lithium carbonate instead of lithium peroxide or oxides expected for $Li^+$-ORR.[10−16] The parasitic reactions between the ORR intermediates and the carbonate-based solvents can greatly influence the discharge voltages and hamper the development of highly active catalysts for $Li^+$-ORR in stable electrolytes necessary for rechargeable Li-air batteries.

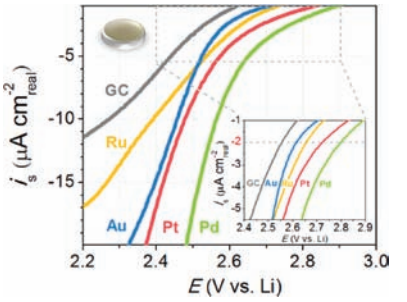


**Figure 1.** Background- and IR-corrected specific ORR polarization curves of polycrystalline Pd, Pt, Ru, Au, and GC surfaces in $O_2$-saturated 0.1 M $LiClO_4$ in DME at 100 rpm and 20 mV $s^{-1}$.

In this study, we have performed systematic ORR studies on four different polycrystalline metal catalysts, palladium (Pd), platinum (Pt), ruthenium (Ru), and gold (Au), as well as glassy carbon (GC) via rotating-disk electrode (RDE) in 0.1 M $LiClO_4$ in 1,2-dimethoxyethane (DME). Previous studies on ORR electrocatalysis in aqueous electrolytes have shown that the activity can be governed by the oxygen binding to the catalyst surface.[17−20] In this report, the activity trend for $Li^+$-ORR on these surfaces is correlated with oxygen adsorption energy, which can serve as a predictive tool for the design and screening of highly active catalysts. In addition, the activity trend obtained on these polycrystalline surfaces translates well to that of high-surface-area thin-film catalysts supported on GC electrode via RDE and early discharge voltages of the Li-$O_2$ cells.

DME was used as the solvent to study the ORR activity, as it is reasonably stable during ORR, unlike carbonate-based solvents.[6,10,21,22] The stability of DME in the operation window in this study (3.1 to 2.0 $V_{Li}$) is within the stable window of DME reported by Aurbach et al. (4.5 to 1.0 $V_{Li}$ on Pt).[23] In addition, Figure S1 in the Supporting Information (SI) shows that there is no significant reaction current associated with Pt, oxygen, and DME in the potential range of 3.1 to 2.0 $V_{Li}$, and the $O_2/O_2^{-\bullet}$ redox couple is stable and reversible on Pt electrode in DME. Furthermore, it does not poison Pt for ORR, and DME has minimal interactions with the Pt surfaces (Figure S2), unlike PC shown in our previous work.[24] All the RDE measurements reported herein were collected from a three-electrode cell with $O_2$-saturated 0.1 M $LiClO_4$ ion DME (Novelyte USA, $H_2O$ <20 ppm) in a water-free glovebox ($H_2O$ < 0.1 ppm, $O_2$ < 1%).

**Received:** September 12, 2011
**Published:** November 01, 2011

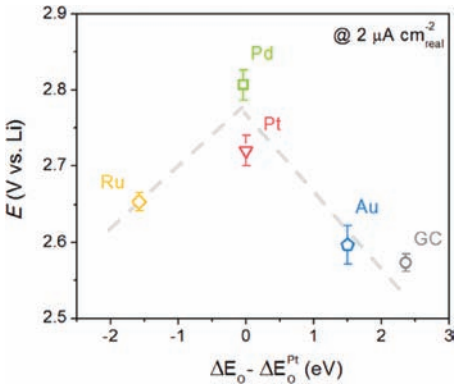


**Figure 2.** Nonaqueous $Li^+$-ORR potentials at 2 $\mu A\ cm^{-2}_{real}$ as a function of calculated oxygen adsorption energy, $\Delta E_O$ (per oxygen atom relative to an atom in the gas phase),[25] relative to that of Pt. The oxygen adsorption energy on GC is estimated from the oxygen adsorption energy on graphite.[26] Error bars represent standard deviations of at least three independent measurements.

All electrodes were vacuum-dried at 75 °C for at least 12 h, followed by direct transfer from the vacuum oven to the water-free glovebox without exposure to the ambient. Detail experimental conditions for all RDE measurements and electrode preparation can be found in the SI.

The real-surface-area-normalized ORR current densities of the five bulk surfaces, termed specific activity ($i_s$, $\mu A\ cm^{-2}_{real}$), are shown in Figure 1, which was obtained after background and IR corrections (SI and Figure S3). The real surface area of each bulk surface was estimated from electrochemical measurements (details in the SI).

The $Li^+$-ORR activity was found to be Pd > Pt > Ru ≈ Au > GC. As these surfaces exhibited similar Tafel slopes of ~150 mV per decade up to 2 $\mu A\ cm^{-2}_{real}$ (not shown), the dashed line in Figure 1 inset shows that the intrinsic activity for each surface can be assessed by the potential to achieve a given specific ORR current density. For Pd, Pt, Ru, Au, and GC, the specific activity of 2 $\mu A\ cm^{-2}_{real}$ can be reached at a potential of 2.80 (±0.02), 2.72 (±0.02), 2.65 (±0.01), 2.60 (±0.03), and 2.57 (±0.01) $V_{Li}$, respectively. It should be noted that this specific current at the scan rate of 20 mV $s^{-1}$ corresponds to the self-poisoning of less than 10% of one monolayer solid $LiO_2$ formation (200 $\mu C\ cm^{-2}_{real}$),[21] and the background-current correction less than 50% of the total ORR current (Table S1).

The intrinsic $Li^+$-ORR activities of the five surfaces exhibit a volcano shape as a function of the oxygen adsorption energy relative to that of Pt (per oxygen atom relative to an atom in the gas phase),[25,26] as shown in Figure 2. The activity increases from GC to Au, followed by Pt, and peaks at Pd as the oxygen adsorption energy increases. A further increase in the oxygen adsorption energy on Ru results in a decrease in the activity compared to the peak (Pd), forming a so-called "volcano-type" relationship. This volcano dependence suggests that the strength of oxygen binding on the catalyst surface greatly influences the ORR activity, at least in the present case of submonolayer coverages with discharge product. It should be noted that the ORR potential for GC in Figure 2 is lower than those typically found for carbon in the Li-$O_2$ cells. This difference can be attributed at least in part to the fact that the specific current of 2 $\mu A\ cm^{-2}_{real}$, which is constrained by ORR surface poisoning and background current correction, is much higher than those typically used in the Li-$O_2$ cells (~0.1−0.2 $\mu A\ cm^{-2}_{carbon}$).[2,7,9,27]

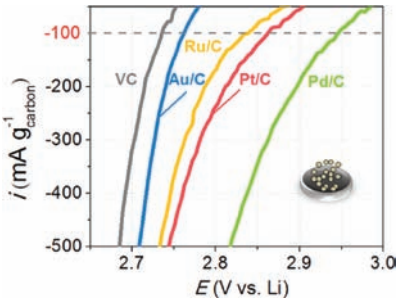


**Figure 3.** Background- and IR-corrected ORR polarization curves of Pd/C, Pt/C, Ru/C, Au/C, and VC thin films on GC (0.05 $mg_{carbon}\ cm^{-2}_{disk}$) in $O_2$-saturated 0.1 M $LiClO_4$ in DME at 900 rpm and 5 mV $s^{-1}$.

To bridge the intrinsic $Li^+$-ORR activity trends on the bulk surfaces to the discharge voltages of Li-$O_2$ cells, the activities of high-surface-area catalysts supported on Vulcan carbon (VC with 40% metal catalyst loading, Premetek, USA; SI pp S4−S6) were examined subsequently using RDE measurements. The weight percent of metal loading is defined as the weight of metal normalized to the weight of metal and carbon (metal/metal + C). We used a method developed recently[28,29] for the quantitative evaluation of the activities of high-surface-area catalysts dispersed as thin films on a GC RDE, where mass-transport resistances were negligible. Figure 3 shows the background- and IR-corrected ORR current densities of Pd/C, Pt/C, Ru/C, Ru/C, Au/C, and VC thin films normalized to carbon weight. It should be noted that current densities shown here are comparable to those typically used in the Li-$O_2$ cells (~100−500 mA $g^{-1}_{carbon}$).[2,7,9] For Pd/C, Pt/C, Ru/C, Au/C, and VC, the ORR activity of 100 mA $g^{-1}_{carbon}$ can be reached at a potential of 2.95, 2.86, 2.84, 2.76, and 2.74 $V_{Li}$, respectively. This is in agreement with the fact that, at ~100 mA $g^{-1}_{carbon}$, the ORR voltage on carbon estimated from the RDE data in Figure 3 is ~2.7 $V_{Li}$, very consistent with those reported in a large number of Li-air cell studies.[2,7,9] With further consideration of estimated true surface area of each catalyst (SI pp S5−S6), the specific ORR current densities (Figure S4) of high-surface-area catalysts are in reasonable agreement with the activity trend of bulk surfaces shown in Figure 2. It should be noted that the specific current range evaluated for these high-surface-area catalysts (Figure S4) is comparable to those used typically in Li−$O_2$ cells (~0.1−0.5 $\mu A\ cm^{-2}_{catalyst}$).[2,7,27]

We further show that the ORR activity trends found on bulk surfaces and high-surface-area catalysts from RDE measurements can be translated well to the discharge voltage trends of Li-$O_2$ cells. All the Li-$O_2$ cells were tested in the water-free glovebox. All the air electrodes and separators (Celgard, C480) were vacuum-dried at 75 °C for at least 12 h prior to being transferred into an Ar-filled, water-free glovebox ($H_2O$ < 0.1 ppm, $O_2$ < 0.1 ppm). The electrodes and the separators were kept in the vacuum oven and directly transferred to the glovebox without exposure to the ambient. The Li-$O_2$ cell consists of lithium foil, two Celgard separators, and 150 $\mu L$ of $O_2$-saturated 0.1 M $LiClO_4$ in DME as the electrolyte. The composition and weight of the $O_2$ electrode are available in the SI (p S7). To minimize the self-poisoning effect, the initial discharge voltage profiles were used to access the activities of the catalysts as shown in Figure 4;

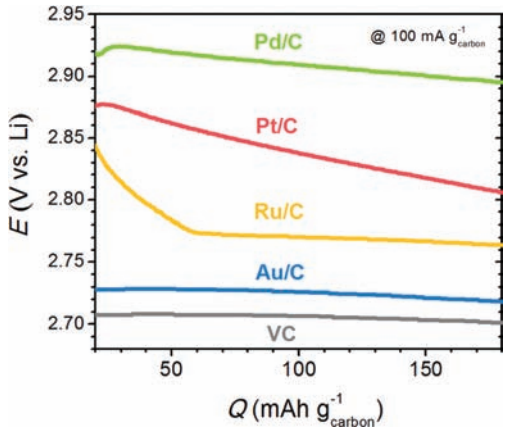


**Figure 4.** Initial discharge profiles of Li-$O_2$ cells of Pd/C, Pt/C, Ru/C, Au/C, and VC at 100 mA $g^{-1}_{carbon}$.

full discharge profiles are shown in Figure S5. The initial discharge voltages of the Li-$O_2$ cells were compared to those found in the high-surface-area thin-film RDE at 100 mA $g^{-1}_{carbon}$ (Figure 3) as shown in Figure S6, confirming a good agreement between the two methods.

The observed volcano-type ORR activity trend on these surfaces is in agreement with the mechanism we proposed previously[24] (Figure S7) and several previous studies.[12,30−32] In nonaqueous electrolytes, the first electron reduction most likely proceeds by the formation of superoxide species such as $O_2^-$ and $LiO_2$. Recently, Peng et al.[12] have provided direct evidence that $O_2$ is reduced to $O_2^-$ on Au and then reacts with $Li^+$, forming $LiO_2$ as an intermediate. On surfaces with weak binding with oxygen, such as Au and GC, $LiO_2$ may disproportionate[12] or undergo a second electron reduction to form $Li_2O_2$, which has been detected in the discharged porous electrodes with carbon[6,10,33] and Au/C[6] electrodes from Li-$O_2$ cells. On surfaces with increasing binding energy with oxygen, such as Pt and Pd (moving left for the right branch of the volcano in Figure 2), it is proposed that the kinetics of the second electron reduction is enhanced to form $Li_2O + O_{adsorbed}$,[24] similar to what has been established for the ORR on Pt and Pt alloy metals in aqueous electrolytes,[19] where $O_{adsorbed}$ subsequently undergoes additional two-electron reduction to form $Li_2O$.[24,34] On further increasing the binding energy of oxygen on surfaces such as Ru, adsorbed oxygen species may bind very strongly on the surface to hamper subsequent electron transfer, leading to reduced ORR activity (left volcano branch). It is interesting to note that the nonaqueous $Li^+$-ORR activity trend observed in this study is well-correlated to that for alkaline ORR, as shown in Figure S8. Further studies involving in situ differential electrochemical mass spectrometry and surface-enhanced Raman spectroscopy[10−12] are needed to verify the proposed mechanism.

In summary, we show that the $Li^+$-ORR activity is in order of Pd > Pt > Ru ≈ Au > GC on bulk surfaces. Such a trend can be translated well to that of high-surface-area thin-film catalysts supported on GC electrodes and early discharge voltages of Li-$O_2$ cells. Oxygen adsorption energy on the surface can greatly influence $Li^+$-ORR activities and form a volcano dependence, which may be used to design highly active ORR surfaces and electrodes with high discharge voltages for Li-air batteries.

## ■ ASSOCIATED CONTENT

**Supporting Information.** Stability of $O_2/O_2^-$ redox couple on Pt in DME, poisoning effect of DME, experimental procedures of all RDE measurements and the raw data, background correction and self-poisoning evaluation, determination of the roughness factors of the bulk disks and the electrochemical surface area of high-surface-area catalysts, ORR polarization curves normalized by the true surface areas of catalyst on the high-surface-area catalysts, Li-$O_2$ single-cell testing, full discharge profiles of Li-$O_2$ single cells, voltage comparison between high-surface-area RDE and the Li-$O_2$ cells, previously proposed ORR mechanism,[24] and ORR activity comparison in nonaqueous and alkaline electrolytes. This material is available free of charge via the Internet at http://pubs.acs.org.

## ■ AUTHOR INFORMATION

### Corresponding Authors

shaohorn@mit.edu; hubert.gasteiger@tum.de

### Present Addresses

[§]Department of Chemistry, Technische Universität München, Lichtenbergstr. 4, D-85747 Garching, Germany

## ■ ACKNOWLEDGMENT

This work was supported by the Assistant Secretary for Energy Efficiency and Renewable Energy, Office of FreedomCAR and Vehicle Technologies of the DOE (DE-AC03-76SF00098 with LBNL) and the Ford-MIT Alliance. This research made use of the Shared Experimental Facilities supported by the MRSEC Program of the National Science Foundation under award no. DMR-0819762. The authors thank Koffi P. C. Yao for assisting with Li-$O_2$ cell design and testing.

## ■ REFERENCES

(1) Bruce, P. G. *Solid State Ion.* **2008**, *179*, 752.
(2) Debart, A.; Paterson, A. J.; Bao, J.; Bruce, P. G. *Angew. Chem., Int. Ed.* **2008**, *47*, 4521.
(3) Ogasawara, T.; Debart, A.; Holzapfel, M.; Novak, P.; Bruce, P. G. *J. Am. Chem. Soc.* **2006**, *128*, 1390.
(4) Girishkumar, G.; McCloskey, B.; Luntz, A. C.; Swanson, S.; Wilcke, W. *J. Phys. Chem. Lett.* **2010**, *1*, 2193.
(5) Wagner, F. T.; Lakshmanan, B.; Mathias, M. F. *J. Phys. Chem. Lett.* **2010**, *1*, 2204.
(6) Lu, Y.-C.; Kwabi, D. G.; Yao, K. P. C.; Harding, J. R.; Zhou, J.; Zuin, L.; Shao-Horn, Y. *Energy Environ. Sci.* **2011**, *4*, 2999.
(7) Lu, Y.-C.; Xu, Z. C.; Gasteiger, H. A.; Chen, S.; Hamad-Schifferli, K.; Shao-Horn, Y. *J. Am. Chem. Soc.* **2010**, *132*, 12170.
(8) Thapa, A. K.; Ishihara, T. *J. Power Sources* **2011**, *196*, 7016.
(9) Debart, A.; Bao, J.; Armstrong, G.; Bruce, P. G. *J. Power Sources* **2007**, *174*, 1177.
(10) McCloskey, B. D.; Bethune, D. S.; Shelby, R. M.; Girishkumar, G.; Luntz, A. C. *J. Phys. Chem. Lett.* **2011**, *2*, 1161.
(11) Freunberger, S. A.; Chen, Y. H.; Peng, Z. Q.; Griffin, J. M.; Hardwick, L. J.; Barde, F.; Novak, P.; Bruce, P. G. *J. Am. Chem. Soc.* **2011**, *133*, 8040.
(12) Peng, Z.; Freunberger, S. A.; Hardwick, L. J.; Chen, Y.; Giordani, V.; Barde, F.; Novak, P.; Graham, D.; Tarascon, J.-M.; Bruce, P. G. *Angew. Chem., Int. Ed.* **2011**, *50*, 6351.
(13) Veith, G. M.; Dudney, N. J.; Howe, J.; Nanda, J. *J. Phys. Chem. C* **2011**, *115*, 14325.
(14) Xu, W.; Xiao, J.; Wang, D. Y.; Zhang, J.; Zhang, J. G. *J. Electrochem. Soc.* **2010**, *157*, A219.

(15) Mizuno, F.; Nakanishi, S.; Kotani, Y.; Yokoishi, S.; Iba, H. *Electrochemistry* **2010**, *78*, 403.
(16) Xiao, J.; Hu, J. Z.; Wang, D. Y.; Hu, D. H.; Xu, W.; Graff, G. L.; Nie, Z. M.; Liu, J.; Zhang, J. G. *J. Power Sources* **2011**, *196*, 5674.
(17) Greeley, J.; Stephens, I. E. L.; Bondarenko, A. S.; Johansson, T. P.; Hansen, H. A.; Jaramillo, T. F.; Rossmeisl, J.; Chorkendorff, I.; Norskov, J. K. *Nat. Chem.* **2009**, *1*, 552.
(18) Lima, F. H. B.; Zhang, J.; Shao, M. H.; Sasaki, K.; Vukmirovic, M. B.; Ticianelli, E. A.; Adzic, R. R. *J. Phys. Chem. C* **2007**, *111*, 404.
(19) Nørskov, J. K.; Rossmeisl, J.; Logadottir, A.; Lindqvist, L.; Kitchin, J. R.; Bligaard, T.; Jonsson, H. *J. Phys. Chem. B* **2004**, *108*, 17886.
(20) Stamenkovic, V. R.; Mun, B. S.; Arenz, M.; Mayrhofer, K. J. J.; Lucas, C. A.; Wang, G. F.; Ross, P. N.; Markovic, N. M. *Nat. Mater.* **2007**, *6*, 241.
(21) Aurbach, D.; Daroux, M. L.; Faguy, P.; Yeager, E. *J. Electroanal. Chem.* **1991**, *297*, 225.
(22) Mitchell, R. R.; Gallant, B. M.; Thompson, C. V.; Shao-Horn, Y. *Energy Environ. Sci.* **2011**, *4*, 2952.
(23) Aurbach, D.; Gofer, Y. In *Nonaqueous electrochemistry*; Aurbach, D., Ed.; CRC Press: New York, 1999; p 200.
(24) Lu, Y.-C.; Gasteiger, H. A.; Crumlin, E.; McGuire, J. R.; Shao-Horn, Y. *J. Electrochem. Soc.* **2010**, *157*, A1016.
(25) Hammer, B.; Norskov, J. K. *Adv. Catal.* **2000**, *45*, 71.
(26) Sorescu, D. C.; Jordan, K. D.; Avouris, P. *J. Phys. Chem. B* **2001**, *105*, 11227.
(27) Park, C. K.; Park, S. B.; Lee, S. Y.; Lee, H.; Jang, H.; Cho, W. I. *Bull. Kor. Chem. Soc.* **2010**, *31*, 3221.
(28) Lu, Y.-C.; Gasteiger, H. A.; Shao-Horn, Y. *Electrochem. Solid State Lett.* **2011**, *5*, A70.
(29) Suntivich, J.; Gasteiger, H. A.; Yabuuchi, N.; Shao-Horn, Y. *J. Electrochem. Soc.* **2010**, *157*, B1263.
(30) Hassoun, J. H. J.; Croce, F.; Armand, M.; Scrosati, B. *Angew. Chem., Int. Ed.* **2011**, *50*, 2999.
(31) Laoire, C. O.; Mukerjee, S.; Abraham, K. M.; Plichta, E. J.; Hendrickson, M. A. *J. Phys. Chem. C* **2009**, *113*, 20127.
(32) Sawyer, D. T.; Chiericato, G.; Angelis, C. T.; Nanni, E. J.; Tsuchiya, T. *Anal. Chem.* **1982**, *54*, 1720.
(33) Laoire, C. O.; Mukerjee, S.; Plichta, E. J.; Hendrickson, M. A.; Abraham, K. M. *J. Electrochem. Soc.* **2011**, *158*, A302.
(34) Xu, Y.; Shelton, W. A. *J. Chem. Phys.* **2010**, *133*, 024703.